Numerical Study of Rotational Effects on Wind Turbines

I. Herráez, B. Stoevesandt*, J. Peinke**
ForWind - University of Oldenburg, Institute of Physics, Oldenburg, Germany,
ivan.herraez@forwind.de;
*Fraunhofer IWES Oldenburg, Germany;
**ForWind - University of Oldenburg, Institute of Physics, Oldenburg, Germany;

Summary

The existence of rotational effects on rotating blades is known since nearly 70 years ago. Many efforts have been done for characterizing them and explaining their physics since their discovery by Himmelskamp. Rotational effects are known to delay the point of stall onset and to increase the maximum lift at high angles of attack. However, the origin of rotational effects is still poorly understood and the models that have been created for their characterization are rather unsatisfactory. In the current work we make use of computational fluid dynamics simulations for shedding some light on the physical mechanisms governing the flow effects provoked by the blade rotation. The knowledge gained from the computations offers valuable information for the development of physically-sound correction models.

1. Introduction

Rotational effects, also commonly referred to as rotational augmentation, were first studied by Himmelskamp [4]. In his experiments on airplane propellers in the 1940s, he observed lift enhancement and stall delay in rotating blades as compared to non-rotating blades. A rotating and a non-rotating wind turbine blade were compared experimentally by Ronsten [5], concluding that rotational augmentation was significant only in the proximity of the hub. Wood [11] observed stall delay to highly depend on the local solidity of the blades. An experimental work by Sicot et al. [8] on a wind turbine with a rotor diameter of 1.37 m compared sectional surface pressure distributions from a rotating and a non-rotating blade operating in turbulent flow. The root region of the blade presented enhanced lift, but no evidence of stall delay was observed. Computational Fluid Dynamics (CFD) simulations have also been commonly used since the last decade for the analysis of rotor aerodynamics. Sørensen et al. [9] performed RANS simulations of the NREL Phase VI Rotor and found increased lift and drag at inboard blade sections. The enhancement of aerodynamic forces was related to radial pumping of the separated flow in the inner blade region. Another numerical and experimental study of the same turbine by
Schreck et al. [7] attributed rotational augmentation to stationary vortical structures located on the upper blade surface. As shown above, current knowledge about rotational effects is still incomplete and requires further investigation if rotor blades are to be designed in a more reliable way. The present work addresses this problem using the MEXICO measurement data set [2] in conjunction with a CFD model based on the open-source CFD toolbox OpenFOAM [1].

2. Methods

2.1. The MEXICO Experiment
The EU FP5 MEXICO (Model EXperiments In COntrolled COnditions) [6] project involved the extensive measuring of loads, surface pressure and PIV flow data of a three bladed 4.5 m rotor diameter wind turbine placed in the Large Low-Speed Facility of the German-Dutch Wind tunnel DNW, which has an open Section of 9.5 x
9.5 m². The design of the blades was based on 3 different aerodynamic profiles: DU91-W2-250 from 20% to 50% radius, RISØ-A1-21 from 54% to 70% radius and

NACA 64-418 from 74% radius to the tip. In this work only a free-stream wind speed of 24 m/s is considered. The rotational speed and pitch angle are kept constant at 424.4 rpm and - 2.3°, respectively. These operating conditions correspond to stalled flow. The flow is aligned with the rotor axis in order to isolate the rotational effects from other influences like dynamic stall. The chord-based Reynolds number varies between 3.5×10^5 and 7×10^5 depending on the wind speed and the blade region. The tip speed is 100 m/s for all cases, meaning a tip speed ratio of 6.7 at design conditions (15 m/s). Further details about the experimental set-up can be found in [2].

2.2. Numerical method and computational mesh

The numerical results presented in this work have been obtained from incompressible steady state Reynolds Averaged Navier-Stokes (RANS) simulations performed with the open source software OpenFOAM. The rotation of the system was accomplished using a non-inertial reference frame and adding the Coriolis and centrifugal forces to the momentum equations. The SIMPLE algorithm was employed for the pressure-velocity coupling. The convective terms were discretized with a second order linear-upwind scheme. The simulations were run fully turbulent and made use of the Spalart and Allmaras [10] turbulence model. Adaptive wall functions were applied for reducing the number of cells in the boundary layer. The wind speed at the inlet and the pressure at the outlet were set to Dirichlet boundary conditions. Atmospheric pressure was predefined at the outlet. Non-slip boundary conditions were set for the blades and the nacelle. For the wind speed at the outlet and the pressure at the inlet Neumann conditions were used.

3. Results and discussion

Figure 1 shows the plane where the flow field was captured 10° after the blade passage by means of PIV measurements. As it can be seen from the picture, the PIV measurements are only available for the outer region of the blade. The CFD results complement the experimental results by providing information about the flow in the inner part of the blade.

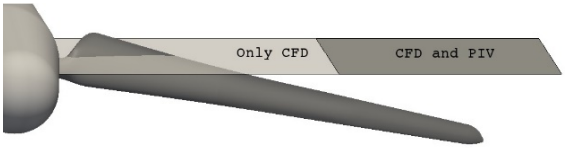

Figure 1: Schematic view of the plane where the flow field was measured 10 after the blade passage. The PIV windows only cover the outboard region, whereas the CFD results encompass the whole blade span.

Figure 2 displays the experimental and numerical results of the flow field at a freestream wind speed of 24 m/s (stall conditions). The agreement between experimental and numerical results for the axial and the radial velocity components is quite good considering the difficulty associated to the prediction of stalled flows. As it can be seen, the blade passage induces a substantial radial flow in the rotor plane. The numerical results indicate that this radial flow is very strong in the inner region of the blade. Two possible sources of radial flows have been mentioned in the literature:

i) Spanwise pressure gradients
ii) The centrifugal force acting on the separated volume of air

In order to elucidate which of both effects is causing the radial flows in the MEXICO turbine, the direction of the velocity vectors is compared with the pressure gradients in Figure. 3. As it can be seen, the radial flows present no connection between the flow direction and the pressure gradients. Therefore, it can be concluded that the source of the radial flows must be the centrifugal force. The flow over the region with separated flow, which is pumped outwards by the centrifugal force, is in fact also subjected to a Coriolis force. The Coriolis force pushes the flow downstream in the chordwise direction, i.e. towards the trailing edge. This effect counteracts the

adverse pressure gradient on the suction side of the blade root, helping to keep the

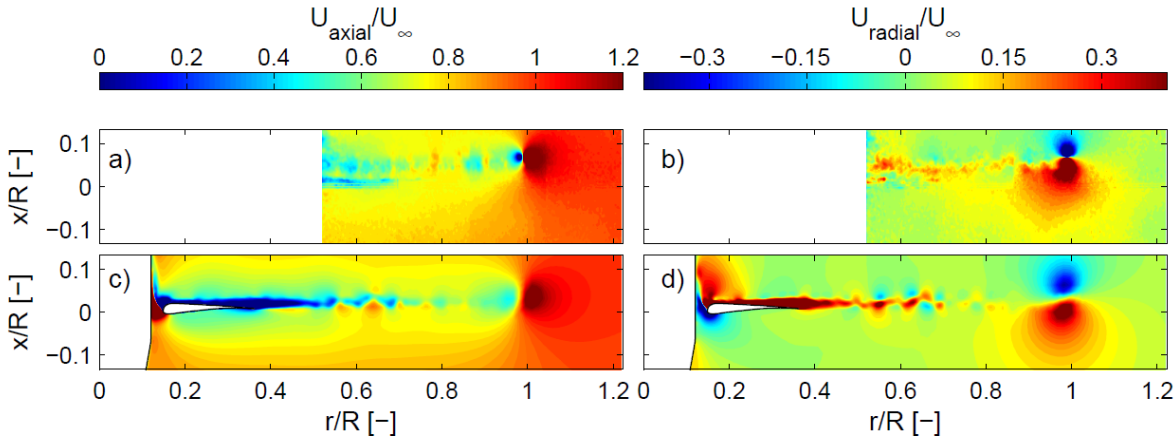

Figure 2: Measured and computed flow field at U∞ = 24 m/s. Upper row: experimental results, lower row: numerical results, left column: axial wind speed, right column: radial wind speed

Flow attached to the blade and correspondingly creating a stall delay effect. This effect can be recognized in the chordwise distribution of the pressure coefficient in Figure 4, where experimental and numerical data obtained from the radial position r=0.25R are compared with 2D airfoil data. As it can be seen, the suction peak is higher in the case of the 3D data and the adverse pressure gradient is strongly reduced as compared to the 2D case, what implies that the flow remains longer attached to the blade. The angle of attack at this conditions is 26° and the sectional lift coefficient of the blade is Cl ≈ 2. This implies that rotational effects lead to an increase of Cl in the blade root of approximately 60% with respect to the 2D airfoil. The interested reader is referred to reference [3] for a deeper insight into the explained flow phenomena.

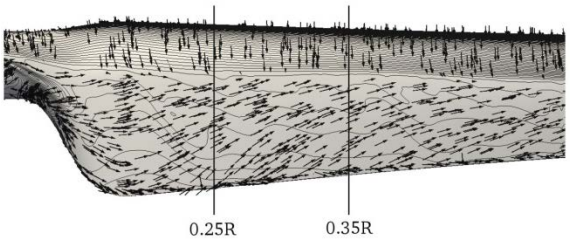

Figure 3: Computed isobars of surface pressure and arrows indicating the flow direction at U∞ = 24 m/s. The isobars go from 0 Pa to 8000 Pa with an interval of 80 Pa. The radial flow in the separated region is mostly unrelated to the pressure gradients.

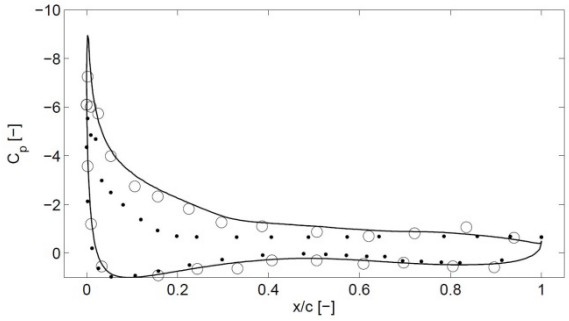

Figure 4: Cp distribution from r = 0.25R for U∞ = 24 m/s, corresponding to AoA = 26°. The dotted line represents 2D experimental results, the circles indicate 3D experimental results and the full line shows 3D numerical results.

4. Conclusions

The MEXICO wind turbine has been simulated by means of a CFD model in order to gain insight into the rotational effects that take place at high angles of attack. The presence of a strong radial flow in the inboard region of the blade was identified both in the experimental and numerical results. The source of the radial flow was attributed to the centrifugal force acting on the separated volume of air. The radial flow is also influenced by a Coriolis force which pushes the flow towards the trailing edge making it to keep longer attached to the blade surface, what provokes a stall delay effect. The subsequent reduction of the adverse pressure gradient enhances significantly the sectional lift.

References

[1] www.openfoam.com.
[2] Boorsma, K., Schepers, J., 2003. Description of experimental setup. MEXICO measurements. Technical Report ECN-X09-0XX. ECN. Petten, Netherlands.
[3] Herr´aez, I., Stoevesandt, B., Peinke, J., 2014. Insight into rotational effects on a wind turbine blade using navierstokes computations. Energies 7, 6798–6822. URL: http://www.mdpi.com/1996-1073/7/10/6798, doi:10.3390/en7106798.
[4] Himmelskamp, H., 1947. Profile investigations on a rotating airscrew. Reports and translations, Volkenrode MAP.
[5] Ronsten, G., 1992. Static pressure measurements on a rotating and a non-rotating 2.375 m wind turbine blade. comparison with 2D calculations. Journal of Wind Engineering and Industrial Aerodynamics 39, 105–118. doi:10.1016/0167-6105(92)90537-K.
[6] Schepers, J., Snel, H., 2007. Model experiments in controlled conditions, final report. Technical Report ECN-E-07-042. ECN. Petten, Netherlands.
[7] Schreck, S.J., Sørensen, N.N., Robinson, M.C., 2007. Aerodynamic structures and processes in rotationally augmented flow fields. Wind Energy 10, 159–178. doi:10.1002/we.214.
[8] Sicot, C., Devinant, P., Loyer, S., Hureau, J., 2008. Rotational and turbulence effects on a wind turbine blade. investigation of the stall mechanisms. Journal of Wind Engineering and Industrial Aerodynamics 96, 1320–1331. doi:10.1016/j.jweia.2008.01.013.
[9] Sørensen, N.N., Michelsen, J.A., Schreck, S., 2002. NavierStokes predictions of the NREL phase VI rotor in the NASA Ames 80 ft 120 ft wind tunnel. Wind Energy 5, 151–169. doi:10.1002/we.64.
[10] Spalart, P.R., Allmaras, S.R., 1994. A one-equation turbulence model for aerodynamic flows. La Recherche Aerospatiale 1, 5–21.
[11] Wood, D., 1991. A three-dimensional analysis of stall-delay on a horizontal-axis wind turbine. Journal of Wind Engineering and Industrial Aerodynamics 37, 1– 14. doi:10.1016/0167-6105(91)90002-E.